

# On the Stability and Realizability of Recurrent Polynomial Surrogate Ternary Logic Gate Networks

Sai Sandeep Damera, Ryan Matheu, Aniruddh G. Puranic, John S. Baras and Calin Belta

**Abstract**—Recurrent Neural Networks (RNNs) can learn to predict Signal Temporal Logic (STL) verdicts online from partial trajectories, but deploying them as runtime monitors in safety-critical systems demands more than predictive accuracy. When sensor inputs degrade or become unavailable, standard architectures such as RNNs offer no structural guarantee that their outputs degrade gracefully; a dropped input can silently flip a verdict from safe to unsafe. We introduce the Recurrent Differentiable Ternary Logic Gate Network (R-DTLGN), a recurrent architecture that operates over Kleene’s three-valued logic  $\{-1, 0, +1\}$ , where 0 explicitly represents *unknown*. The R-DTLGN trains through continuous polynomial surrogates and hardens to a discrete ternary logic circuit at inference. We analyze the hardened circuit through two gate vocabularies derived from two orderings on the ternary domain: numerically monotone gates ensure stable recurrent dynamics, while information-monotone gates, when present, guarantee principled abstention (unknown inputs never produce wrong outputs) and monotonicity in input certainty (more information can only improve the verdict). We show that the recurrent connections required by bounded STL operators use exclusively AND and OR, which belong to both vocabularies, linking the monitoring task’s structure to the architecture’s guarantees. A realizability bound derived from the STL formula’s temporal operators directly sizes the network’s hidden state, replacing hyperparameter search with a formula-driven specification. We evaluate these results on STL specifications over D4RL PointMaze navigation data, testing prediction accuracy, degradation behavior under predicate dropout, and the accuracy-versus-safety tradeoff between two label construction pipelines. The R-DTLGN is, to our knowledge, the first recurrent architecture that couples learned temporal prediction with formal degradation guarantees rooted in three-valued logic.

## I. INTRODUCTION

Monitoring a safety specification online requires evaluating temporal properties as data arrives. Signal Temporal Logic (STL) [1] provides a formal language for such properties over real-valued signals, and its quantitative robustness semantics assign a continuous score measuring the degree of satisfaction or violation. For bounded temporal operators (e.g.,  $\square_{[0,5]} \mu_{\text{safe}}$ ), the ground-truth robustness at time  $t$  depends on signal values up to  $t+5$ , which a causal monitor cannot observe. Tools such as STLGG++ [2] compute the exact robustness offline; when restricted to the available observations, they define a non-learned baseline that can evaluate only the portion of the specification whose temporal horizon has already elapsed.

The gap between this causal baseline and the oracle (full-trajectory) evaluation is fundamental: it exists for every bounded formula with a non-trivial future time horizon. Any

The authors are with the University of Maryland, College Park, USA. Emails: {sdamera, rmatheu, puranic, baras, calin}@umd.edu.

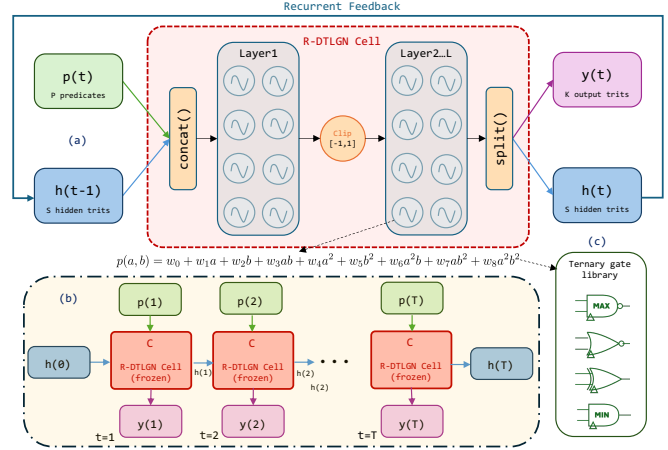


Fig. 1: Schematic of the Recurrent Differentiable Ternary Logic Gate Network. (a) The R-DTLGN cell. (b) Unrolled cell. (c) Hardening into Logic Circuit.

learned monitor attempts to bridge this gap by exploiting spatio-temporal patterns in training data to predict verdicts that a causal evaluator cannot resolve from the available observations alone. Standard recurrent architectures such as LSTM and GRU can serve this role, but they provide no structural guarantees about what happens when input information degrades. Their continuous-valued hidden states carry no inherent distinction between “determined” and “uncertain,” so degraded inputs (sensor dropout, indeterminate predicates) can produce arbitrarily wrong outputs.

Kleene’s strong three-valued logic [3] is the natural formalism for reasoning about temporal properties under partial information. It extends classical Boolean logic with a third value, 0, representing “unknown.” The Kleene connectives (AND, OR, NOT) propagate this unknown value conservatively: a conjunction with one false input is false regardless of the other, but a conjunction of true and unknown yields unknown. This conservative propagation is precisely what a monitor operating under input uncertainty should exhibit.

A learned monitor that operates natively in Kleene’s three-valued domain acquires two complementary capabilities. First, like any learned monitor, it exploits temporal patterns in training data to *predict* verdicts that a causal evaluator cannot resolve; this prediction capability is what makes it useful over the causal baseline. Second, unlike standard recurrent architectures, it provides structural *degradation guarantees*: when input information is lost (predicates become indeterminate, sensors fail), the monitor’s verdicts degrade toward “unknown” rather than flipping to wrong answers. The prediction capability bridges the causal gap; the degradation

guarantee ensures robustness to input-level uncertainty. These two capabilities are complementary and non-overlapping.

We propose the Recurrent Differentiable Ternary Logic Gate Network (R-DTLGN) as a learned monitor that operates natively in Kleene’s domain. Differentiable Logic Gate Networks (DLGNs) [4], [5] replace conventional arithmetic neurons with discrete two-input logic gates, producing pure logic circuits at inference. Polynomial Surrogate Training (PST) [6] extends DLGNs to Kleene’s ternary domain  $\mathbb{T} = \{-1, 0, +1\}$  by representing each neuron as a degree-(2, 2) polynomial with 9 learnable coefficients; at inference, the network *hardens* to an exact ternary logic circuit (Section III-D). The R-DTLGN augments this feedforward architecture with a persistent hidden state for temporal reasoning: at each timestep the cell ingests the current predicate values and its previous state, processes them through  $L$  layers of ternary PST gates, and produces an updated state and output verdict. The hidden state is initialized to  $(0, \dots, 0)$ , the all-unknown state, so the monitor begins with no prior commitment. Because every neuron in the hardened circuit is a ternary gate on  $\mathbb{T}$ , the R-DTLGN’s inference-time computation is a composition of Kleene connectives, inheriting the conservative uncertainty propagation that standard RNNs lack.

*Contributions:* We analyze the R-DTLGN as a causal STL monitor and provide four contributions:

**1) The R-DTLGN architecture.** We introduce the Recurrent Differentiable Ternary Logic Gate Network, a recurrent cell whose neurons are degree-(2, 2) polynomial surrogates during training and exact ternary logic gates at inference. Operating natively in Kleene’s three-valued domain, the R-DTLGN combines the predictive capacity of a learned monitor with the conservative uncertainty propagation of ternary logic. We introduce a novel hardening routine for converting the soft learned network into logic gate circuits in the recurrent setting based on trajectory distillation.

**2) Degradation guarantees from Kleene structure.** We prove that R-DTLGN cells composed of information-monotone gates satisfy two per-timestep properties: *principled abstention* (all-unknown inputs produce all-unknown outputs) and *input certainty monotonicity* (replacing a determined input with unknown can only make outputs less determined, never flip them). These properties guarantee graceful degradation under input loss, a structural advantage over standard recurrent monitors.

**3) Realizability bounds from STL formula structure.** Given a bounded STL formula  $\varphi$ , we derive a lower bound  $B(\varphi)$  on the cell’s hidden state dimension, decomposed additively by temporal operator type. This connects STL formula complexity to neural architecture sizing, replacing hyperparameter search with a formula-driven specification.

**4) Empirical validation.** On a suite of 6 bounded STL specifications over PointMaze navigation data, we evaluate both *prediction performance* (R-DTLGN vs. causal STLGG++ vs. vanilla RNN) and *degradation behavior* (predicate dropout experiments confirming principled abstention and input certainty monotonicity in the learned cell).

## II. RELATED WORK

### A. STL Monitoring and the Causal Gap

Offline STL monitoring tools such as Breach [7], S-TaLiRo [8], STLGG++ [2] compute quantitative robustness given the complete signal trajectory. Online monitoring algorithms process the signal incrementally but still require future samples to resolve bounded temporal operators: the robustness of  $\square_{[0,b]} \mu$  at time  $t$  depends on values up to  $t+b$ . Deshmukh et al. [9] formalized robust online monitoring of partial traces, where the monitor may lack sufficient data to determine the Boolean verdict. Several recent approaches train neural networks to predict STL robustness from partial trajectories [10] using LSTM or GRU cells as the recurrent backbone. These learned monitors bridge the causal gap by exploiting spatio-temporal patterns in data, but they lack structural guarantees about their behavior under input degradation.

### B. Three-Valued Logic in Formal Verification

Kleene’s strong three-valued logic [3] extends classical Boolean logic with a third truth value representing “unknown”. Its connectives are the tightest sound extension of Boolean operations to partial information: a conjunction of true and unknown yields unknown, but a conjunction with false yields false regardless of the other operand. This conservative propagation principle has made three-valued logic a standard tool in formal verification, where it arises whenever an abstraction or partial observation leaves the truth value of a proposition undetermined. The algebraic structure is that of a De Morgan lattice [11], with two distinct orderings: a numerical (truth) ordering and an information (knowledge) ordering. The information ordering, where 0 (unknown) is the least element, is the one relevant to degradation analysis. This paper brings the same algebraic structure to *learned* monitors: the R-DTLGN operates natively in Kleene’s domain, inheriting conservative uncertainty propagation as a structural property rather than an approximation artifact.

### C. Differentiable Logic Gate Networks

Differentiable Logic Gate Networks (DLGNs) [4] replace conventional arithmetic neurons with discrete two-input logic gates, training through continuous relaxations of a categorical gate distribution. Each neuron maintains a softmax distribution over the 16 Boolean gates, selecting the mode at inference. Convolutional extensions [5] and subsequent work on connection optimization demonstrate competitive accuracy at extreme parameter efficiency. The softmax-over-gates paradigm is feasible because the Boolean gate space is small ( $2^{2^2} = 16$ ), but it becomes intractable for ternary logic ( $3^{3^2} = 19,683$  gates). Polynomial Surrogate Training (PST) [6] overcomes this via a direct polynomial parameterization (Section III-D), matching binary DLGN accuracy while training 2–7× faster. Bührer et al. [12] introduced recurrent DLGNs for sequential tasks over Boolean values but do not address the hardness fragility that arises in recurrent settings. All prior DLGN work is either feedforward or operates in the binary domain. Our proposed R-DTLGN combines recurrence with the ternary

PST framework, and its dynamics under the information ordering have not been previously analyzed.

*Gap addressed by this work:* No existing learned STL monitor has a structural connection to the three-valued logic that underlies STL semantics under partial information. The R-DTLGN is, to our knowledge, the first learned architecture whose inference-time computation operates natively in Kleene’s three-valued domain, providing provable degradation guarantees that complement its learned prediction capability.

### III. PRELIMINARIES

#### A. Signal Temporal Logic (STL)

A discrete-time signal is a function  $x : \mathbb{N} \rightarrow \mathbb{R}^n$  mapping discrete-time indices to a real-valued system state, where  $\mathbb{N}$  is the set of all nonnegative integers. STL [1] is a modal logic for specifying temporal behaviors of real-valued signals over bounded time intervals. The primitives in STL are *predicate functions*, responsible for mapping a signal to the Boolean domain. A predicate function has the general form  $\mu := f(x(t)) \geq 0$ , where  $f : \mathbb{R}^n \rightarrow \mathbb{R}$  is a continuous function. STL formulas are defined recursively over the following grammar:

$$\varphi := \mu \mid \neg\varphi \mid \varphi_1 \wedge \varphi_2 \mid \square_{[a,b]} \varphi \mid \diamond_{[a,b]} \varphi \mid \varphi_1 \mathbf{U}_{[a,b]} \varphi_2$$

where  $\square_{[a,b]}$  is the unary *always* operator,  $\diamond_{[a,b]}$  is the unary *eventually* operator,  $\mathbf{U}_{[a,b]}$  is the binary *until* operator, and  $[a, b]$  is a bounded time interval with  $a, b \in \mathbb{N}$ ,  $a \leq b$ . For example, the formula  $(x_1(t) \leq 0) \mathbf{U}_{[0,5]} \square_{[0,2]} (x_2(t) \geq 2)$  states that  $x_1$  must remain less than or equal to zero until, within 0 to 5 time steps,  $x_2$  becomes and remains greater than or equal to two for 3 time steps.

The *quantitative robustness*  $\rho(\varphi, x, t) \in \mathbb{R}$  measures the degree of satisfaction at time  $t$ :

$$\begin{aligned} \rho(\mu, x, t) &= f(x(t)), \\ \rho(\neg\varphi, x, t) &= -\rho(\varphi, x, t), \\ \rho(\varphi_1 \wedge \varphi_2, x, t) &= \min(\rho(\varphi_1, x, t), \rho(\varphi_2, x, t)), \\ \rho(\square_{[a,b]} \varphi, x, t) &= \min_{\tau \in [t+a, t+b]} \rho(\varphi, x, \tau), \\ \rho(\diamond_{[a,b]} \varphi, x, t) &= \max_{\tau \in [t+a, t+b]} \rho(\varphi, x, \tau), \end{aligned} \quad (1)$$

A positive robustness ( $\rho > 0$ ) implies satisfaction; a negative robustness ( $\rho < 0$ ) implies violation. The sign of  $\rho$  is sound:  $\text{sign}(\rho(\varphi, x, t)) = +1$  if and only if the Boolean semantics evaluate to true.

For bounded operators, evaluating  $\rho$  at time  $t$  requires signal values up to  $t+b$ . A causal monitor operating at time  $t$  has access only to the available observations  $\{x(0), \dots, x(t)\}$  and therefore cannot compute the oracle robustness for formulas with non-trivial future horizons.

#### B. The Ternary Domain and Its Two Orderings

The ternary domain  $\mathbb{T} = \{-1, 0, +1\}$  admits two natural partial orders with different roles. The numerical ordering governs training-time stability; the information ordering governs inference-time degradation guarantees.

**Definition 1** (Numerical ordering). The *numerical ordering*  $\leq$  on  $\mathbb{T}$  is the restriction of the standard order on  $\mathbb{R}$ :  $-1 \leq 0 \leq +1$ .

This is a total order with bottom  $-1$ , top  $+1$ , meet  $\min$ , and join  $\max$ .

**Definition 2** (Information ordering). The *information ordering* (Kleene ordering)  $\sqsubseteq$  on  $\mathbb{T}$  is defined by:  $0 \sqsubseteq -1$ ,  $0 \sqsubseteq +1$ , with  $-1$  and  $+1$  incomparable. The value 0 represents *unknown* and is the unique bottom element  $\perp = 0$ . The values  $\pm 1$  are maximal but incomparable: they represent different determined values, not different levels of certainty. This is a *flat pointed partially ordered set*: an antichain with a bottom element, but *not* a lattice (the join  $(-1) \vee (+1)$  does not exist).

Both orderings extend componentwise to  $\mathbb{T}^n$ . In particular,  $\mathbb{T}^S$  under  $\sqsubseteq$  has bottom  $\perp = (0, \dots, 0)$  (the “all-unknown” state).

**Definition 3** (Monotonicity under each ordering). A function  $g : \mathbb{T}^2 \rightarrow \mathbb{T}$  is *numerically monotone* if  $a \leq a'$ ,  $b \leq b'$  implies  $g(a, b) \leq g(a', b')$ , and *information-monotone* if  $a \sqsubseteq a'$ ,  $b \sqsubseteq b'$  implies  $g(a, b) \sqsubseteq g(a', b')$ .

The numerical ordering governs the continuous training dynamics: the cell operates on  $[-1, 1]^S$  with real-valued activations, and gradient-based analysis uses the Euclidean structure inherited from  $\mathbb{R}^S$ . The information ordering governs the discrete inference dynamics: after hardening, the cell operates on  $\mathbb{T}^S$  and the relevant structure is the pointed poset  $(\mathbb{T}^S, \sqsubseteq)$  with bottom  $\perp = (0, \dots, 0)$  that distinguishes “unknown” from “determined”.

#### C. Gate Vocabularies

The monotonicity definition (Definition 3) applied under each ordering yields two gate vocabularies with distinct guarantees. Of the  $3^9 = 19,683$  two-input ternary gates, exactly 175 are *numerically monotone* (NM) and exactly 197 are *information-monotone* (IM). Excluding the 3 constant gates leaves 172 NM non-constant and 194 IM non-constant gates.

In a recurrent circuit composed entirely of NM gates, the state-update map is order-preserving on  $[-1, +1]^S$ , so Tarski’s theorem [13] guarantees fixed-point existence and bounded orbits. NM gates are therefore the natural vocabulary for the recurrent path.

$\neg$		$\wedge$	$F$	$U$	$T$	$\vee$	$F$	$U$	$T$
$F$	$T$	$F$	$F$	$F$	$F$	$F$	$F$	$U$	$T$
$U$	$U$	$U$	$F$	$U$	$U$	$U$	$U$	$U$	$T$
$T$	$F$	$T$	$F$	$U$	$T$	$T$	$T$	$T$	$T$

The 197 IM gates include all Kleene strong connectives: NOT, AND, OR (defined above), NAND, NOR; XOR and XNOR under Kleene extension; IMPLIES and its variants; both projections  $\pi_1$  and  $\pi_2$ ; and all three constant gates. IM gates provide the degradation guarantees developed in Section V-B. However, the majority of IM gates have zero-absorbing rows ( $g(0, b) = 0$  for all  $b$ ). A recurrent circuit of pure IM gates cascades toward the all-unknown fixed point, producing degenerate memory.

The two vocabularies overlap at exactly 20 gates (17 non-constant), including AND, OR, both projections, and their complements. Gates in this intersection, denoted  $\text{NM} \cap \text{IM}$ ,

inherit both recurrent stability (from NM) and degradation guarantees (from IM). Section V shows that bounded STL temporal operators require only  $\text{NM} \cap \text{IM}$  gates in their recurrent connections, making this intersection the ideal target vocabulary.

#### D. Polynomial Surrogate Training (PST)

We now define the PST neuron, network architecture, training objective, and hardening procedure used throughout the paper.

a) *PST neuron*: Each two-input ternary gate  $g : \mathbb{T}^2 \rightarrow \mathbb{T}$  is represented by the polynomial  $p_{\mathbf{w}} : \mathbb{R}^2 \rightarrow \mathbb{R}$  defined as:

$$p_{\mathbf{w}}(a, b) = \mathbf{w}^\top \mathbf{m}(a, b), \quad (2)$$

where  $\mathbf{m}(a, b) = [1, a, b, ab, a^2, b^2, a^2b, ab^2, a^2b^2]^\top$  is the monomial basis and  $\mathbf{w} \in \mathbb{R}^9$  are the learnable coefficients. The  $9 \times 9$  Vandermonde matrix  $V$  evaluating these monomials at the grid points  $\mathbb{T}^2$  is invertible, so the mapping between coefficients  $\mathbf{w}$  and truth table values  $\mathbf{t} = V\mathbf{w}$  is a bijection. The polynomial is  $C^\infty$ -smooth and linear in  $\mathbf{w}$ , requiring no softmax temperatures or Gumbel relaxations.

b) *Network architecture*: A feedforward PST-DTLGN is specified by its depth  $L$ , layer widths  $\{n_l\}_{l=0}^L$ , a connectivity map  $\mathbf{C}$  assigning two parents to each neuron, and the polynomial coefficients  $\mathbf{w}_j^{(l)} \in \mathbb{R}^9$  for each neuron  $j$  at layer  $l$ . The forward pass applies a clip nonlinearity after each polynomial evaluation:

$$h_j^{(l)} = \text{clip}\left(p_{\mathbf{w}_j^{(l)}}(h_{s_j}^{(l-1)}, h_{t_j}^{(l-1)})\right), \quad (3)$$

where  $\text{clip}(x) = \max(-1, \min(1, x))$  and  $(s_j, t_j)$  are the parent indices from  $\mathbf{C}$ . Clipping preserves the range  $[-1, 1]$ , prevents polynomial blowup across layers, and preserves the grid points  $\{-1, 0, +1\}$  exactly.

c) *Training*: The training objective combines a task loss with a commitment regularizer that encourages polynomial evaluations at grid points to approach valid ternary values:

$$\mathcal{L}(\mathbf{W}) = \mathcal{L}_{\text{task}}(\mathbf{W}) + \lambda(s) \cdot \mathcal{R}_A(\mathbf{W}), \quad (4)$$

where  $\mathcal{R}_A$  penalizes the distance from each neuron's soft truth table to the nearest valid ternary truth table, and  $\lambda(s)$  is annealed from  $\approx 0$  (free exploration) to  $\lambda_{\text{max}}$  (strong commitment) during training.

d) *Hardening*: At inference, each neuron is converted to a discrete ternary gate: its polynomial is evaluated on the  $3 \times 3$  grid  $\mathbb{T}^2$ , each entry is rounded to the nearest element of  $\mathbb{T}$ , and the resulting truth table is looked up in the gate library. Formally, the hardened coefficients are  $\mathbf{w}_j^{\text{hard}} = V^{-1} \text{round}_{\mathbb{T}}(V\mathbf{w}_j)$ . Since rounding always produces a valid element of  $\mathbb{T}^9$ , every trained PST neuron discretizes to one of the 19,683 possible two-input ternary gates without requiring a curated vocabulary. The hardened network is a pure ternary logic circuit. This works in the feedforward setting but makes the hardening fragile in the recurrent setting, where per-neuron errors amplify in the recurrent loop.

## IV. THE RECURRENT PST-DTLGN

An R-DTLGN cell is parameterized by four integers:  $P$  (input predicates),  $S$  (hidden state trits),  $K$  (output trits), and  $L$  (layer depth), as described in Figure 1. At each timestep  $t$ , the cell receives a predicate vector  $p_t \in \mathbb{R}^P$  and the previous hidden state  $h_{t-1} \in \mathbb{R}^S$ , and produces:

$$z_t = [p_t; h_{t-1}] \in \mathbb{R}^{P+S}, \quad \tilde{h}_t = f^{(L)} \circ \dots \circ f^{(1)}(z_t) \in \mathbb{R}^{S+K}, \\ h_t = \text{clip}(\tilde{h}_t^{(1:S)}, -1, +1), \quad y_t = \tilde{h}_t^{(S+1:S+K)},$$

where each layer  $f^{(\ell)}$  is a collection of two-input PST gates (Section III-D), clip restricts activations to  $[-1, 1]$ ,  $h_t$  is the updated hidden state, and  $y_t$  is the output. The hidden state is initialized to  $h_0 = (0, \dots, 0)$ , the all-unknown state under the information ordering.

During training the cell is differentiable (each gate evaluates its polynomial at continuous values in  $[-1, 1]$ ); at inference, the cell is hardened to an exact ternary logic circuit via trajectory distillation (Section IV-A).

#### A. Recurrent Hardening via Trajectory Distillation

Per-neuron hardening (rounding each polynomial to its nearest gate independently) described in Section III-D is inadequate for recurrent cells: each gate assignment propagates through all subsequent timesteps, and locally optimal rounding produces globally incoherent dynamics.

We replace per-neuron rounding with *trajectory distillation*, a greedy coordinate-descent procedure over a target vocabulary  $\mathcal{V}$ . Given  $N_{\text{cal}}$  calibration trajectories from the training data: (i) generate teacher verdicts  $\hat{y}_t^{(n)} \in \mathbb{T}$  by thresholding the soft network's output; (ii) warm-start the circuit by per-neuron rounding against the full library (19,683 gates); (iii) sweep all gates in output-to-input order, replacing each with the  $\mathcal{V}$ -candidate that minimizes verdict disagreement on the calibration set; (iv) iterate until no sweep improves. Each sweep monotonically decreases disagreement, guaranteeing convergence; 3–7 sweeps suffice in practice.

a) *Two-phase vocabulary refinement*: Restricting  $\mathcal{V}$  directly to the 17 non-constant  $\text{NM} \cap \text{IM}$  gates is too constrained, causing significant accuracy loss. We therefore adopt a two-phase strategy: *Phase 1* sweeps with  $\mathcal{V} = \mathcal{V}_{\text{NM}}$  (172 NM non-constant gates), eliminating the hardening gap and guaranteeing stable dynamics (Section III-C). *Phase 2* attempts to replace each NM-only gate with the nearest  $\text{NM} \cap \text{IM}$  candidate, accepting the swap if accuracy loss is below  $\eta = 0.1$  pp. This upgrades as many gates as possible to the intersection vocabulary, extending degradation guarantees (Section V-B).

#### B. The Causal STL Monitoring Task

Given a bounded STL formula  $\varphi$  and a dataset of trajectories  $\{x^{(n)}\}_{n=1}^N$  with offline robustness labels  $\rho_t^{(n)} = \rho(\varphi, x^{(n)}, t)$ , we seek an R-DTLGN cell that produces ternary verdicts online from the available observations. Concretely, at each timestep  $t$ , the cell observes only the current predicate values  $p_t = (\mu_1(x(t)), \dots, \mu_P(x(t)))$  and its own hidden state

$h_{t-1}$ , and outputs a verdict  $y_t \in \{-1, 0, +1\}$  approximating  $\text{sign}(\rho(\varphi, x, t))$ .

The *causal baseline* is the causal restriction of an exact STL evaluator (e.g., STLCG++ [2]): it computes the standard robustness using only the available observations  $\{x(0), \dots, x(t)\}$ , producing correct verdicts only for formulas whose temporal horizon has fully elapsed. The gap between this baseline and the oracle (full-trajectory) evaluation is the space a learned monitor must exploit. The R-DTLGN’s training objective is a loss on ternary labels derived from the oracle robustness  $\rho_i^{(n)}$ , with two options for label construction described below.

The R-DTLGN is trained on ternary labels derived from the continuous robustness signal, but two legitimate pipelines exist for constructing these labels. The distinction is analogous to the *optimize-then-discretize* (OtD) vs. *discretize-then-optimize* (DtO) choice in numerical methods.

**Compute-then-Quantize (CtQ)** evaluates STL robustness from the continuous predicates, then quantizes the resulting scalar  $\rho$  to a ternary label. **Quantize-then-Compute (QtC)** first rounds each predicate to  $\mathbb{T}$ , then evaluates STL robustness from the ternary predicates. CtQ labels reflect the full continuous-predicate information; QtC labels reflect only what the ternary inputs can structurally determine.

Since ternary rounding is sign-preserving ( $\text{sign}(\bar{\mu}_i) \in \{0, \text{sign}(\mu_i)\}$ ), the two pipelines can disagree only by expanding the unknown region:

**Proposition 1** (QtC sign preservation). *Let  $\bar{\mu}_i : \mathbb{R}^n \rightarrow \mathbb{T}$  be a sign-preserving quantization of each predicate. Then for any bounded STL formula  $\varphi$  with standard min/max semantics, the QtC robustness  $\bar{\rho}$  satisfies  $\text{sign}(\rho) \cdot \text{sign}(\bar{\rho}) \geq 0$ . That is, QtC can only widen the unknown band relative to CtQ; it cannot flip a satisfaction to a violation or vice versa.*

*Proof sketch.* Structural induction on  $\varphi$ . The base case holds by the sign-preserving assumption. For min:  $\rho > 0$  forces both arguments positive, so both quantized arguments are  $\geq 0$ , giving  $\bar{\rho} \geq 0$ .  $\rho < 0$  forces at least one argument negative, giving  $\bar{\rho} \leq 0$ . The max case is symmetric. Bounded temporal operators reduce to finite min/max chains.  $\square$

The CtQ/QtC choice is a design tradeoff between accuracy and safety. CtQ training targets the true verdict but asks the network to commit at timesteps where ternary inputs alone are insufficient to determine the outcome; it relies on the learned temporal patterns to fill the gap. QtC training targets only the structurally recoverable verdicts, aligning the training objective with the degradation guarantees of Section V-B: the network is never asked to produce a verdict that its ternary inputs cannot support.

## V. ANALYSIS

We analyze the hardened R-DTLGN cell (the inference-time ternary circuit). The analysis rests on two gate vocabularies derived from the two orderings of Section III-B: numerically monotone (NM) gates govern recurrent stability, while information-monotone (IM) gates govern degradation

behavior under input loss. We restrict the recurrent path to NM gates to promote stable training dynamics. The analysis here focuses on inference-time properties of the hardened circuit.

### A. STL Structure and the $\text{NM} \cap \text{IM}$ Intersection

**Proposition 2** (STL recurrent operators use  $\text{NM} \cap \text{IM}$  gates). *Standard bounded STL temporal operators require recurrent connections composed exclusively of gates in  $\text{NM} \cap \text{IM}$ . Specifically:  $\square_{[a,b]}$  uses windowed AND (min) over a delay line;  $\diamond_{[a,b]}$  uses windowed OR (max) over a delay line;  $\varphi_1 \mathbf{U}_{[a,b]} \varphi_2$  decomposes into AND/OR combinations with delay-line state. Negation ( $\neg$ ) uses the pointwise NOT gate, which is information-monotone but not numerically monotone; however, STL semantics ensure negation is applied only to predicates in the feedforward path, never within temporal recurrence.*

Proposition 2 establishes that the  $\text{NM} \cap \text{IM}$  vocabulary is expressively sufficient for exact STL monitoring: a faithful implementation *can* be built from these gates alone. The recurrent connections use AND (for  $\square$ :  $h_t = p_t \wedge h_{t-1}$ ) and OR (for  $\diamond$ :  $h_t = p_t \vee h_{t-1}$ ). Negation is pushed to the predicate level by duality ( $\neg \square \varphi \equiv \diamond \neg \varphi$ ), acting in the feedforward path only. The zero-absorbing behavior of AND and OR at unknown inputs is the correct ternary monitoring semantic (an Always monitor receiving unknown input *should* produce unknown). A learned R-DTLGN need not recover this exact structure; the proposition ensures that restricting the gate vocabulary to  $\text{NM} \cap \text{IM}$  does not sacrifice expressiveness for the target task.

**Remark 1** (Expressiveness cost). *Restricting to the 197 IM gates or the 172 NM non-constant gates excludes the vast majority of the 19,683 possible gates, but none of the excluded gates correspond to any standard logic operation needed for STL monitoring. The restriction costs zero expressiveness for the STL monitoring task.*

### B. Degradation Guarantees

We now state the per-timestep properties that information-monotonicity provides. These are properties of *single function evaluations*, not of dynamical trajectories across multiple timesteps. They govern what happens when inputs to a working monitor are lost or degraded. Crucially, these guarantees are conditional: they hold for any subcircuit composed of IM gates, and apply to the full cell only if all gates in the cell are IM.

Let  $F : \mathbb{T}^P \times \mathbb{T}^S \rightarrow \mathbb{T}^S$  denote the hardened R-DTLGN cell’s state-update function, where  $P$  is the number of predicate inputs and  $S$  the number of hidden-state trits.

**Proposition 3** (Principled abstention). *If  $F$  is composed entirely of non-constant information-monotone gates, then  $F(\perp, \perp) = \perp$ . That is, when all predicate inputs are unknown and the hidden state is all-unknown, the cell produces all-unknown outputs. The cell never fabricates a verdict from absent evidence.*

*Proof.* For a non-constant information-monotone gate  $g$ , we have  $g(0, 0) = 0$ : the output at bottom must be at or below all other outputs under  $\sqsubseteq$ , and a non-constant gate cannot map  $\perp$

to a determined value (doing so would require the output to be constant, since  $g(\perp) \sqsubseteq g(a, b)$  for all  $a, b$ ). Composing across all  $L$  layers: each layer receives all-zero inputs and produces all-zero outputs, so the all-unknown state propagates to the output.  $\square$

**Proposition 4** (Input certainty monotonicity). *If  $F$  is composed entirely of information-monotone gates, then for any fixed hidden state  $h \in \mathbb{T}^S$ :*

$$p \sqsubseteq p' \implies F(p, h) \sqsubseteq F(p', h). \quad (5)$$

*Replacing any predicate value with unknown (0) can only make the cell's output less determined, never flip a determined verdict.*

**Remark 2** (Degradation, not prediction). *Propositions 3 and 4 are degradation guarantees: architectural invariants of the IM vocabulary that hold for any learned parameterization. They govern how the monitor behaves when input information is lost, but say nothing about prediction from temporal patterns, which comes from the learned parameters. This separates the R-DTLGN from standard recurrent monitors: in an RNN, degradation behavior is at best encouraged by training (e.g., via dropout augmentation) and depends on the learned weights; in the R-DTLGN it is guaranteed by architecture and independent of them.*

**Remark 3** (Polynomial short-circuit property). *The degradation guarantees hold exactly at ternary grid points. During training, the PST polynomial surrogates preserve this behavior at absorbing inputs: if a gate's truth table has a constant row at grid point  $a^*$ , the degree-(2, 2) interpolant satisfies  $p_g(a^*, b) = c$  for all  $b \in \mathbb{R}$  (a degree-2 polynomial with 3 roots is identically zero). This short-circuit property ensures that the soft network's behavior at ternary inputs matches the hardened cell's, bridging the training and inference phases for the degradation analysis.*

### C. Initialization via Kleene Fixed-Point Theorem

The per-timestep guarantees hold at every evaluation independently. We now examine what can be said about the cell's behavior across multiple timesteps when the gates are information-monotone.

**Theorem 1** (Kleene initialization convergence). *Let  $F$  be composed of information-monotone gates and fix a constant input  $p \in \mathbb{T}^P$ . Define  $G_p(h) = F(p, h)$ . Then  $G_p$  is monotone on the finite pointed poset  $(\mathbb{T}^S, \sqsubseteq)$ , and the Kleene ascending chain from the all-unknown state converges to the least fixed point:*

$$\perp \sqsubseteq G_p(\perp) \sqsubseteq G_p^2(\perp) \sqsubseteq \dots \sqsubseteq G_p^k(\perp) = h^* \quad \text{for some } k \leq S.$$

*The bound  $k \leq S$  holds because each strict step promotes at least one component from 0 to  $\pm 1$ , and information-monotonicity prevents a determined component from reverting to unknown.*

*Proof.* The partially ordered set  $(\mathbb{T}^S, \sqsubseteq)$  is finite and possesses a unique bottom element  $\perp = (0, \dots, 0)$ .  $G_p$  is monotone

by the same argument as Proposition 4 (monotonicity in  $h$  for fixed  $p$ ). By Kleene's fixed-point theorem for monotone maps on finite pointed domains, the ascending chain from  $\perp$  converges to the least fixed point in at most  $S$  steps (the height of the lattice).  $\square$

*Scope and practical interpretation.*: Theorem 1 assumes constant input  $p$  and convergence from  $\perp$ . From non- $\perp$  states, convergence is not guaranteed: IM gates can produce limit cycles (the gate NOT satisfies  $\text{NOT}(0) = 0$ , so  $\perp$  is a fixed point, but generates a period-2 cycle  $+1 \rightarrow -1 \rightarrow +1 \rightarrow \dots$  from determined states, since  $+1$  and  $-1$  are incomparable under  $\sqsubseteq$ ). The initialization  $h_0 = \perp$  is therefore a requirement, not merely a convention.

The constant-input assumption is more permissive than it appears. After ternary quantization, predicates encoding semantically stable conditions (“the agent is safe,” “the agent has reached the goal”) produce piecewise-constant input sequences whose plateaus typically span many sampling periods. During each plateau, Theorem 1 guarantees convergence to the least fixed point within  $S$  steps; when a predicate transitions, the per-timestep guarantees of Propositions 3–4 continue to hold during the transient. This characterization weakens for predicates that chatter near a quantization threshold.

### D. Minimum State Dimension

We now ask: given a bounded STL formula, how large must the R-DTLGN cell be? The question has classical precedents: the Myhill-Nerode theorem relates language complexity to minimum automaton state count, and the Kalman minimal realization theorem relates input-output behavior to minimum state dimension in linear systems. We derive an analogous result for the R-DTLGN.

**Definition 4** (State complexity). For a bounded STL formula  $\varphi$ , define the *state complexity*  $B(\varphi)$  recursively. Let  $w = b - a + 1$  denote the interval width:

$$\begin{aligned} B(\mu) &= 0, \\ B(\neg\varphi) &= B(\varphi), \\ B(\varphi_1 \wedge \varphi_2) &= B(\varphi_1) + B(\varphi_2), \\ B(\Box_{[a,b]} \varphi) &= w + B(\varphi), \\ B(\Diamond_{[a,b]} \varphi) &= w + B(\varphi), \\ B(\varphi_1 \mathbf{U}_{[a,b]} \varphi_2) &= 2w + B(\varphi_1) + B(\varphi_2). \end{aligned} \quad (6)$$

Disjunction is treated identically to conjunction.

The intuition is straightforward. Atomic predicates require no memory (they are external inputs). Negation is pointwise and adds no state. Conjunction and disjunction require independent buffers for each subformula. Each temporal operator maintains a shift register of length  $w$  over the subformula's recent evaluations; Until requires two such registers (one per operand).

**Theorem 2** (Minimum state dimension). *Any R-DTLGN cell capable of computing the monitoring function for a bounded STL formula  $\varphi$  requires hidden state dimension  $S \geq B(\varphi)$ .*

*Proof sketch.* The monitoring function must distinguish all signal prefixes that lead to different future monitoring states. Each temporal operator with interval  $[a, b]$  requires a shift register of length  $w$  to store the subformula’s recent evaluations, and the cell’s ternary state components are the only available memory between timesteps. The registers for distinct operators in the parse tree must be maintained independently. The additive total across the parse tree gives  $B(\varphi)$ .  $\square$

**Remark 4** (Necessity, not sufficiency). *The bound  $S \geq B(\varphi)$  is necessary: a cell with  $S < B(\varphi)$  lacks sufficient memory. It does not claim that  $S = B(\varphi)$  suffices. The gap between necessity and sufficiency arises from the two-input gate topology, which introduces routing overhead.*

### E. Computational Depth Bound

The state complexity  $B(\varphi)$  bounds the memory (hidden state dimension) required across timesteps. A complementary bound governs the per-timestep computation: how many layers of PST gates are needed to update all sliding windows and produce the current output?

**Proposition 5** (Per-timestep depth). *For a bounded STL formula  $\varphi$  with nesting depth  $d$  and maximum interval length  $k_{\max} = \max_{[a,b] \in \varphi} (b-a+1)$ , the minimum layer count satisfies*

$$L \geq d \cdot \lceil \log_2 k_{\max} \rceil. \quad (7)$$

Together, Theorem 2 and Proposition 5 characterize the minimum cell dimensions:  $S \geq B(\varphi)$  gives the width (hidden state), and  $L \geq d \cdot \lceil \log_2 k_{\max} \rceil$  gives the depth (layers). For the specification  $\varphi_1 = \mu_{\text{safe}} \mathbf{U}_{[0,5]} \mu_{\text{goal}}$  ( $w = 6, d = 1$ ):  $B(\varphi_1) = 12$  and  $L \geq \lceil \log_2 6 \rceil = 3$ .

## VI. RESULTS

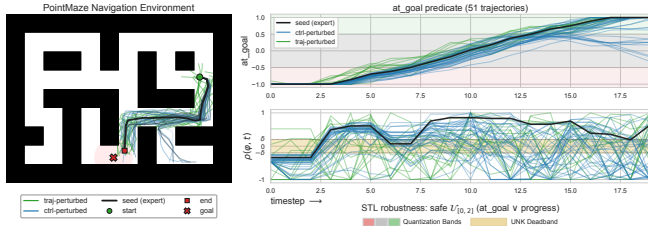


Fig. 2: Experimental setup for the navigation case.

We evaluate the R-DTLGN on 816 trajectories ( $T = 20$ ) from the D4RL PointMaze Large maze [14], generated by perturbing seed trajectories through physics-based resimulation and selected to ensure balanced ternary label coverage ( $\delta = 0.20$ ). Five predicates are defined over  $x(t) = [q, \dot{q}]$ :  $\mu_g$  (at goal),  $\mu_s$  (safe),  $\mu_m$  (moving),  $\mu_h$  (heading toward goal),  $\mu_p$  (approach rate), each normalized to  $[-1, +1]$ .

We construct 6 bounded STL specifications over these predicates (Table I), spanning 2–4 predicates with closed-prefix Until semantics. All temporal horizons satisfy  $w \leq 4$ . Each R-DTLGN cell is sized from the realizability bound:  $S = B(\varphi)$  hidden-state trits,  $L = 6$  layers (Theorem 2, Proposition 5), replacing hyperparameter search with formula-driven architecture sizing.

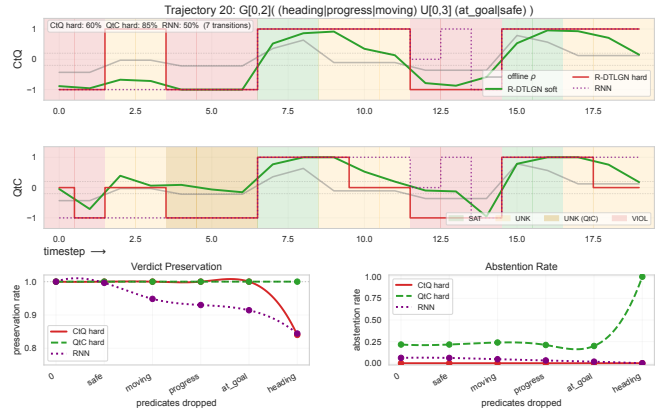


Fig. 3: S06 ( $P=5$ ), Trajectory 20: verdict traces (top: CtQ, middle: QtC) and per-predicate progressive dropout (bottom). The QtC hard circuit maintains perfect verdict preservation across all dropout levels while abstention increases monotonically (Props. 3–4); the RNN shows degrading preservation with no abstention mechanism. Background shading: green = SAT, yellow = UNK, red = VIOL.

Each model is trained with NM-enforced PST ( $\lambda_{\max} = 0.3$ ) under both label construction pipelines (CtQ and QtC), then hardened via two-phase trajectory distillation (Section IV-A) using the training set as calibration data. A vanilla RNN (Elman network) with matched hidden dimension is trained on CtQ labels as a baseline.

a) *Crossing the causality gap:* The nested temporal structure creates a large gap between what a causal evaluator can resolve and what the monitoring task requires: the causal STLGG++ baseline averages 38.2% across the 6 specifications, with values as low as 29.9% (S03). Both the R-DTLGN and the RNN bridge this gap through learned temporal patterns. On S02, the CtQ hard circuit reaches 76.7% against a causal floor of 43.7%, a 33 pp improvement; on S06, the CtQ hard circuit reaches 71.7% against 33.8%, a 38 pp improvement. CtQ matches or exceeds the RNN on four of six specifications (S02, S03, S04, S06), while operating in a discrete ternary domain that admits structural degradation analysis.

b) *Hardening and distillation:* Two-phase trajectory distillation (Section IV-A) converts the soft PST network to a hardened ternary circuit. The hardening gap varies substantially across specifications: CtQ loses less than 2 pp on S02 and S03, while QtC loses 22.5 pp on S01 (from 77.9% soft to 55.4% hard). On S06, both pipelines show a negative hardening gap (hard exceeds soft), suggesting distillation acts as a regularizer for that specification. NM  $\cap$  IM gate compliance after the second distillation sweep ranges from 76–86%, with higher compliance generally correlating with smaller accuracy loss. The hardened circuit is a pure ternary logic network with no floating-point arithmetic, directly realizable as an ASIC.

c) *Degradation behavior:* We evaluate input-certainty monotonicity (Proposition 4) on the distilled circuits through two tests. *Verdict preservation* measures the fraction of timesteps where masking a single predicate to 0 does not flip the verdict sign. *Lattice monotonicity* tests the full proposition across all  $2^P$  predicate subsets. The proposition predicts 100% for both metrics on fully IM cells; in practice, NM  $\cap$  IM compliance after distillation ranges from 76–86%,

**TABLE I:** Evaluation across 6 STL specifications ( $T=20, L=6, S=B(\varphi)$ ). **Prediction:** *Causal* is the non-learned STLGG++ baseline restricted to available observations; *RNN* is a vanilla Elman network; *CtQ/QtC* are hard R-DTLGN circuits after two-phase distillation (soft accuracy in parentheses). **Preservation:** mean verdict preservation under single-predicate dropout (Prop. 4 predicts 1.0 for IM cells). **Lattice:** compliance with input-certainty monotonicity across all  $2^P$  predicate subsets; for each subset pair  $A \subset B$ , the less-informed verdict must either abstain or agree with the more-informed verdict (Prop. 4 predicts 100% for fully IM cells). Not applicable to the RNN.

Specification	Task	$P$	$S$	Causal	Prediction (%)			Preservation (%)			Lattice (%)	
					CtQ	QtC	RNN	CtQ	QtC	RNN	CtQ	QtC
S01 $\square_{[0,3]}(\mu_h \mathbf{U}_{[0,3]} \mu_g)$	head $\rightarrow$ goal	2	12	45.4	67.7 (67.7)	55.4 (77.9)	73.4	89.3	100.0	90.0	81.0	100.0
S02 $\square_{[0,2]}((\mu_h \vee \mu_p) \mathbf{U}_{[0,3]} \mu_g)$	approach $\rightarrow$ goal	3	11	43.7	76.7 (78.7)	76.6 (75.9)	76.5	89.2	88.7	92.8	81.0	80.3
S03 $\square_{[0,2]}((\mu_h \vee \mu_s) \mathbf{U}_{[0,3]} (\mu_g \vee \mu_p))$	safe $\rightarrow$ arrive	4	11	29.9	68.8 (69.0)	64.4 (71.1)	66.9	93.3	100.0	91.0	92.3	100.0
S04 $\square_{[0,2]}((\mu_h \vee \mu_p) \mathbf{U}_{[0,3]} (\mu_g \vee \mu_s))$	approach $\rightarrow$ safe	4	11	46.2	73.2 (74.1)	55.8 (74.9)	71.5	88.7	95.3	91.3	78.3	91.1
S05 $\square_{[0,2]}((\mu_h \vee \mu_s) \mathbf{U}_{[0,3]} \mu_g) \wedge \diamond_{[0,3]}(\mu_p \vee \mu_m)$	safe $\rightarrow$ goal + move	5	15	30.1	61.0 (67.8)	61.3 (63.6)	70.3	92.9	96.4	88.5	85.9	87.0
S06 $\square_{[0,2]}((\mu_h \vee \mu_p \vee \mu_m) \mathbf{U}_{[0,3]} (\mu_g \vee \mu_s))$	active $\rightarrow$ safe	5	11	33.8	71.7 (71.0)	70.4 (69.4)	69.7	96.8	100.0	94.2	93.9	99.7
<b>Mean</b>				38.2	69.8	64.0	71.4	91.7	96.7	91.3	85.4	93.0

so deviations are expected and observed.

*Preservation* is the more consistent result. QtC achieves  $\geq 88.7\%$  preservation on every specification, reaching 100% on S01, S03, and S06. CtQ preservation ranges from 88.7% to 96.8%, with a mean of 91.7%. In both cases, the R-DTLGN is competitive with the RNN (88–94%), with QtC exceeding the RNN on five of six specifications.

*Lattice monotonicity* tests Proposition 4 across the full power-set lattice of predicate subsets (all  $2^P$  combinations), not just single-predicate dropout. For every pair of subsets  $A \subset B$ , the verdict under  $A$  must either abstain or agree with the verdict under  $B$ ; violations indicate that removing information flipped a determined verdict. QtC achieves 93.0% mean lattice compliance, reaching 100% on two specifications (S01, S03) and 99.7% on S06. CtQ averages 85.4%, reflecting the weaker unknown-signal coverage in CtQ training labels. This metric has no RNN analogue: the information ordering underlying the lattice test is specific to the ternary domain and does not apply to continuous-valued networks.

Figure 3 illustrates the full degradation profile on S06 ( $P=5$ ), which achieves the highest compliance and the clearest separation between pipelines. The QtC circuit maintains perfect preservation across all dropout levels and transitions to full abstention at blackout. The CtQ circuit preserves 96.8% of verdicts but produces 0% abstention, reflecting sparser unknown coverage in CtQ training labels. The RNN degrades steadily (94.2% preservation, no abstention).

The CtQ and QtC pipelines occupy distinct points in the accuracy-assurance tradeoff. CtQ approaches or matches RNN-level accuracy but loses the structural degradation advantages that distinguish the R-DTLGN from a standard recurrent network. QtC preserves those advantages more reliably, at the cost of a larger hardening gap on some specifications. In both cases, the preservation behavior is *guaranteed by architecture* for the IM-compliant portion of the cell, not merely *encouraged by training* as would be required for an RNN to exhibit similar behavior through dropout augmentation.

## VII. CONCLUSION

We analyzed the R-DTLGN as a causal STL monitor and identified two structural advantages rooted in its native operation in Kleene’s three-valued domain. First, cells composed of

information-monotone gates guarantee graceful degradation under input loss: principled abstention and input certainty monotonicity ensure that verdicts degrade toward “unknown” rather than flipping to wrong answers when predicates become indeterminate. Second, the STL formula’s temporal operator structure determines a lower bound on the cell’s hidden state dimension, replacing hyperparameter search with formula-driven architecture sizing.

These two capabilities complement the R-DTLGN’s role as a learned monitor. Like any neural architecture trained on robustness labels, the R-DTLGN exploits spatio-temporal patterns to predict verdicts that a causal evaluator cannot resolve from the available observations alone. The Kleene connection adds a layer of structural assurance: the prediction capability bridges the causal gap, and the degradation guarantee ensures robustness to input-level uncertainty.

*Limitations and future work:* The degradation guarantees require information-monotone gates; two-phase distillation improves but does not fully close the hardening gap. Three directions follow: gated R-DTLGN variants for longer temporal horizons, multi-trit encodings to break the quantization bottleneck, and DFA extraction for formal model checking of the learned circuit.

## REFERENCES

- [1] O. Maler and D. Nickovic, “Monitoring temporal properties of continuous signals,” in *International symposium on formal techniques in real-time and fault-tolerant systems*. Springer, 2004, pp. 152–166.
- [2] P. Kapoor, K. Mizuta, E. Kang, and K. Leung, “Stlcc++: A masking approach for differentiable signal temporal logic specification,” *IEEE Robotics and Automation Letters*, 2025.
- [3] M. Fitting, “Kleene’s three valued logics and their children,” *Fundamenta informaticae*, vol. 20, no. 1-3, pp. 113–131, 1994.
- [4] F. Petersen, C. Borgelt, H. Kuehne, and O. Deussen, “Deep differentiable logic gate networks,” *Advances in Neural Information Processing Systems*, vol. 35, pp. 2006–2018, 2022.
- [5] F. Petersen, H. Kuehne, C. Borgelt, J. Welzel, and S. Ermon, “Convolutional differentiable logic gate networks,” *Advances in Neural Information Processing Systems*, vol. 37, pp. 121 185–121 203, 2024.
- [6] S. S. Damera, R. Matheu, A. G. Puranic, and J. S. Baras, “Polynomial surrogate training for differentiable ternary logic gate networks,” *arXiv preprint arXiv:2603.00302*, 2026.
- [7] A. Donz , “Breach, a toolbox for verification and parameter synthesis of hybrid systems,” in *International Conference on Computer Aided Verification*. Springer, 2010, pp. 167–170.

- [8] Y. Annpureddy, C. Liu, G. Fainekos, and S. Sankaranarayanan, "S-taliro: A tool for temporal logic falsification for hybrid systems," in *International Conference on Tools and Algorithms for the Construction and Analysis of Systems*. Springer, 2011, pp. 254–257.
- [9] J. V. Deshmukh, A. Donzé, S. Ghosh, X. Jin, G. Juniwal, and S. A. Seshia, "Robust online monitoring of signal temporal logic," *Formal Methods in System Design*, vol. 51, no. 1, pp. 5–30, 2017.
- [10] M. Ma, J. Gao, L. Feng, and J. Stankovic, "Stlnet: Signal temporal logic enforced multivariate recurrent neural networks," *Advances in Neural Information Processing Systems*, vol. 33, pp. 14 604–14 614, 2020.
- [11] R. Cignoli, "Injective de morgan and kleene algebras," *Proceedings of the American Mathematical Society*, pp. 269–278, 1975.
- [12] S. Bühner, A. Plesner, T. Aczel, and R. Wattenhofer, "Recurrent deep differentiable logic gate networks," *arXiv preprint arXiv:2508.06097*, 2025.
- [13] A. Tarski, "A lattice-theoretical fixpoint theorem and its applications." 1955.
- [14] J. Fu, A. Kumar, O. Nachum, G. Tucker, and S. Levine, "D4rl: Datasets for deep data-driven reinforcement learning," *arXiv preprint arXiv:2004.07219*, 2020.